Aeolian Research 18 (2015) 145–153

Contents lists available at ScienceDirect

Aeolian Research

journal homepage: www.elsevier.com/locate/aeolia

Variable effects of saltation and soil properties on wind erosion of different textured soils

F. Avecilla [a], J.E. Panebianco [a], D.E. Buschiazzo [b,*]

[a] INCITAP (CONICET-UNLPam), Argentina
[b] INTA Anguil, INCITAP (CONICET-UNLPam), Argentina

ARTICLE INFO

Article history:
Received 31 March 2015
Revised 23 July 2015
Accepted 23 July 2015

Keywords:
Wind erosion
Saltation
Impact energy
Degree of structure
Soil properties

ABSTRACT

Wind erosion largely depends on saltation. Nevertheless, the effect of the composition of the saltation fraction of different textured soils is poorly understood, as is the relative influence of both saltation and soil properties on wind erosion. In order to answer these questions, wind erosion of six differently textured soils were simulated with a wind tunnel. The following saltation conditions were considered: injected saltation, in which the saltation fraction of each soil was added to the soil bed; no saltation, in which the soil eroded naturally, without injection of its saltation fraction; and only saltation, in which the saltation fraction was injected in absence of the soil bed. Results indicated that total erosion amounts increased as a function of the abrasion energy of the saltating particles but also with decreasing aggregation rate of the saltation fraction. The aforementioned agrees with a lower aggregate stability and higher amounts of the erodible fraction of sandy soils. Though saltation of individual sand grains produced impacts of higher kinetic energy on the soil surface of sandy soils than of fine textured soils, the relative erosion (quotient between the erosion occurred with and without saltation) was higher in finest soils, indicating a larger effect of saltation, probably due to the larger fragmentation of aggregates in these soils. Results of this study indicated that both the composition of the saltating fraction and also the intrinsic properties of the soil determined wind erosion.

1. Introduction

The magnitude of wind erosion has been mostly attributed to the saltation movement (Bagnold, 1941) based on the fact that saltating particles fall on the soil surface, transferring their momentum and mobilizing new particles to the air (Dong et al., 2002). Because of this, the relationship between saltation and wind erosion has been frequently studied. Many of these studies used pure quartzite sands that resemble, in shape, micro solid spheres (Bauer et al., 2004; Cheng et al., 2009; Creyssels et al., 2009). Shao et al. (1993a,b) found that the abrasion of a surface is related to the diameter of the saltating particles, which determines the kinetic energy of each impact. Dietrich (1977) and Greeley et al. (1982) concluded that the key parameters in controlling abrasion are the kinetic energy of the particles impacts and the bonding strength of the eroded material, and that the amount of material mobilized by the impact of a particle is a function of its diameter and transportation speed (Bridges et al., 2005).

The use of pure sand as the saltating material allowed a good understanding of the mechanics of the saltation process and the elucidation of the relationship between saltation and wind erosion. Nevertheless, the use of this kind of saltator partially reflects the real situation in soil, whose/which saltation fraction can be composed of individual particles but also aggregates. As a matter of fact, Alfaro (2008) mentions that when the saltation fraction is composed mainly of individual mineral particles, the energy that is triggered on the soil surface is higher than when it is composed of aggregates. He attributed this difference to the higher density of mineral particles than of aggregates, which are frequently formed by low dense organic substances. Hagen (1984, 1991) and Hagen et al. (1988) found that the abrasion of aggregates by saltating particles was proportional to the kinetic energy of these abrasive particles, and that soil losses caused by the use of soil aggregates is 10% higher than when sand is used as an abrader. Other authors have mentioned that the relationship between saltation and wind erosion varies as a function of soil texture. Grini and Zender (2004) showed that coarse-textured soils contained more saltators with high kinetic energy than fine-textured soils. Rice and McEwan (2001) suggested that the amount of eroded soil increases exponentially as the proportion of fine materials in the soil decrease.

The particle size distribution is a frequently used parameter in the classic approach for wind erosion modeling (Marticorena and

* Corresponding author.

http://dx.doi.org/10.1016/j.aeolia.2015.07.005
1875-9637/© 2015 Published by Elsevier B.V.

Bergametti, 1995; Shao et al., 1996; Alfaro et al., 1997; Alfaro and Gomes, 2001) but the effects of the composition of the saltation fraction on wind erosion rate is generally not considered. Under this approach, it can be expected that soils with a saltation fraction that comprises a higher proportion of low density aggregates, and hence lower kinetic energy, will produce less mass when exposed to increased saltation than sandy soils. On the other hand, it can be supposed that aggregates that are less cohesive can also be broken in subsequent finer fractions. This will result in larger amounts of transportable material and hence, will produce more successive impacts, increasing the wind erosion process in a non linear way and augmenting the total mass transported downwind. The rupture of aggregates during the wind erosion process was generally analyzed and discussed in the context of dust emission (Shao, 2008; Kok et al., 2012) but less information is available on the influence of the aggregation rate of saltating particles on wind erosion amounts.

The interaction between the magnitude of saltation and the characteristics of the soil surface on wind erosion has not been studied in detail. At this point, the following question is stated: under comparable wind erosion conditions, do sandy soils erode more than fine textured soils due to the higher saltation energy of their saltators or because of their higher susceptibility to be eroded by wind?. It is widely known that sandy soils are more erodible than fine textured, because of their lower binding effect between individual particles, which produces higher amounts of erodible fraction (López et al., 2007). Ta (2007) found that the rate of abrasion of the soil is proportional to the impact energy and inversely proportional to the contents of the fine materials of the soil.

The aim of this study was to analyze, in soils of variable textures, the effect of both, the characteristics of the soil surface and the composition of its saltation fractions on wind erosion amounts.

2. Materials and methods

2.1. Soil sampling and analysis

Six soils placed along a north–south transect were analyzed within the semiarid area of central Argentina. The selected soils had variable textures: between sandy and loamy (Table 1 and Fig. 1). The classification of the soil textural classes was made according to USDA (Soil Survey Division Staff, 1993).

Undisturbed soil samples were taken from the first 2.5 cm topsoil. A portion of the sample was air-dried and hand sieved through 2 mm in order to homogenize it. Another subsample was air dried and sieved with a rotary sieve (Chepil, 1962). This device is a rotating nest of concentric cylindrical sieves with 0.42, 0.84, 2.0, 6.4 and 19.2 mm square openings. With this method the percentage of the <0.84 mm size aggregates, the erodible fraction of the soil (EF), was calculated with the following equation (Colazo and Buschiazzo, 2010):

$$EF = \frac{W < 0.84}{TW} \times 100 \quad (1)$$

where EF is the erodible fraction (%), $W < 0.84$ is the weight (g) of <0.84 mm aggregates, and TW is the initial weight (g) of total sample.

The dry aggregate stability (DSS)) was calculated after a second dry sieving of each aggregate size (Skidmore et al., 1994) using Eq. (2),

$$DSS = \left[1 - \frac{W < 0.84_2}{W > 0.84_1}\right] \times 100 \quad (2)$$

where $W < 0.84_2$ is the weight (g) of aggregates that went through the 0.84 mm sieve after a second sieving and $W > 0.84_1$ is the weight (g) of aggregates retained on the 0.84 mm sieve after the first sieving.

The saltation fraction of each soil (0.2–0.5 mm, van Pelt et al., 2010) was separated manually by dry sieving. The textural composition of each saltation fraction was determined by means of the wet sieving and pipette method (Schlichting et al., 1995). This analysis was carried out on dispersed and less-dispersed samples, allowing an estimation of the aggregation state of each soil, which was achieved by calculating the relative variation of the clay fraction (<0.002 mm) between the two dispersion pre-treatments. Dispersion treatments included the destruction of free carbonates (with 6% acetic acid) and organic matter (with hydrogen peroxide), a dispersion with sodium hexametaphosphate, the agitation in water for 30 min at 1500 rpm, and an ultrasound treatment at 35 kHz for 15 min. The less dispersed sample was only agitated in water for 30 min at 100 rpm.

A relative soil aggregation index (RSI)) of the saltation fraction was obtained by means of Eq. (3),

$$RSI = clay * OM \quad (3)$$

where clay is the percentage of the <2 μm – sized fractions of the soils determined with the pipette method, and OM the organic matter contents of the soil. The use of this coefficient was based on the consideration that both soil components are the main factors affecting soil aggregation in soils (Perfect et al., 1995; Mirzamostafa et al., 1998).

The grain size distribution of the saltation fraction of each soil was also determined with a laser particle counter Malvern Mastersizer Model 2000 (Fig. 2). This method allowed a more precise determination of the grain size distribution than the pipette

Table 1
Main characteristics of the studied soils.

SOIL		S1	S2	S3	S4	S5	S6
Geographical coordinates		36° 33′S 64° 18′W	39° 23′S 62° 37′W	33° 40′S 65° 22′W	36° 34′S 63° 59′W	36° 32′S 64° 17′W	36° 35′S 63° 57′W
Textural class		Sand	Loamy sand	Loamy sand	Loamy sand	Sandy loam	Loam
	Clay (<0.002 mm)	49.9	92.5	82	74.9	102.3	171.6
Grain size distribution	Silt (0.002–0.053 mm)	67.3	99.7	124.2	124	186.2	355.5
(g kg^{-1})	Very fine sand I (0.053–0.074 mm)	87.2	55.2	230.6	69.6	135.8	129.3
	Very fine sand II (0.074–0.105 mm)	176.2	80.7	366.9	191.7	180.8	129.1
	Fine sand (0.105–0.250 mm)	543.2	569.4	171.9	287.2	342.1	173
	Medium and coarse sand (0.250–2 mm)	76.2	102.5	24.4	252.6	52.8	41.5
	Clasts (>2 mm) (%)	0	6.7	0	0	0	0
OM (g kg^{-1})		13.7	20.8	7	18.4	13.1	28.2
$CaCO_3$ (g kg^{-1})		5.5	6.5	8.7	5.5	4.3	8.8
EF (%)		71.6	84.3	79.1	57.5	49.5	21.2
DSS (%)		62.2	82	54.4	80.7	85.7	95.7

OM = organic matter; EF = erodible fraction, DSS = dry aggregate stability.

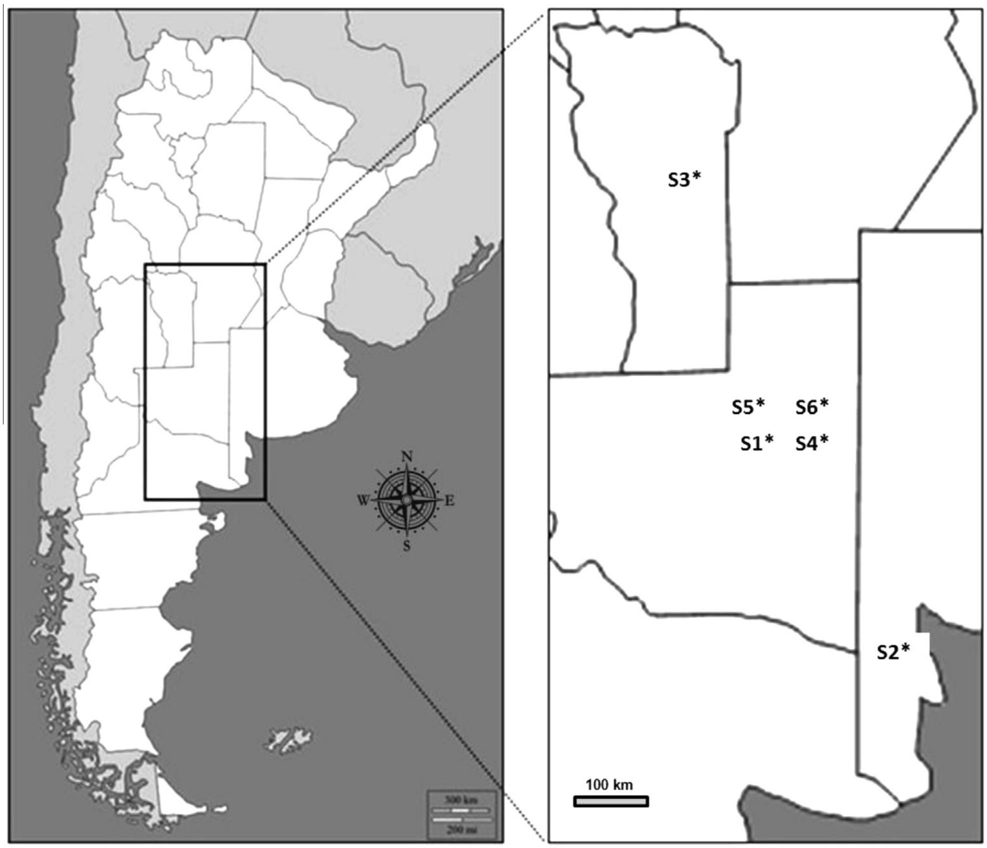

Fig. 1. Location of the studied soils.

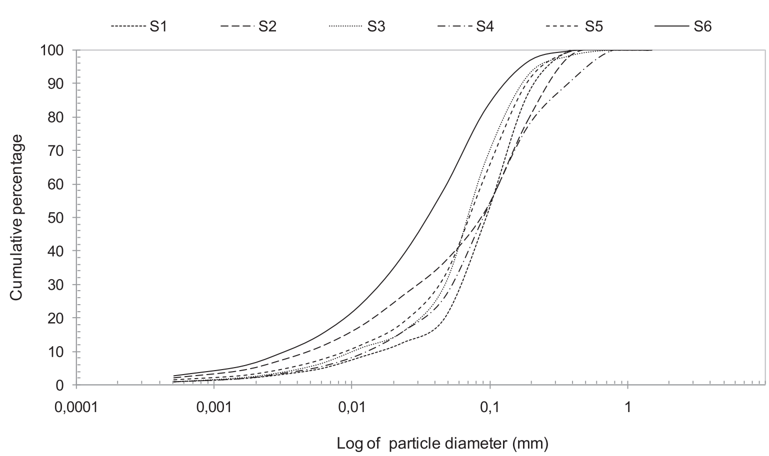

Fig. 2. Grain size distribution of the saltation fraction of the studied soils.

method, and was only used for a more detailed characterization of the composition of this fraction. The grain size distribution was obtained from non dispersed samples. The geometric mean diameter (GMD), the size fraction at 50% of the cumulative distribution of the particle size distribution curve, was determined for each saltation fraction.

In order to determine the energy of the saltating fraction of each soil, a Sensit device (Stockton and Gillette, 1990) was placed at 0.05 m height above the soil surface, at the end of the wind tunnel working section. Measurements were carried out during each simulation test at 1 s. intervals. Though, it existed a good general positive correlation between Sensit pulses and wind erosion (R^2: 0.51; $p < 0.001$), results of Sensit measurements were not consistent, due to the fact that this device did not record any energy in some cases in which wind erosion existed or it measured energy in absence of wind erosion. Similar variable results were detected by other authors (Baas, 2004; Barchyn and Hugenholtz, 2010; Barchyn et al., 2014). The aforementioned situation lead us to take the decision of not using the Sensit energy records in this study and to determine the energy of the saltating fraction by means of other available methodologies. The abrader energy of the saltating fraction was therefore determined with Eq. (4),

$$E = 0.5 \times m \times \mu_p^2 \quad (4)$$

where E is the abrader energy in joules, m is the mass (g) and μ_p is the measured average speed of the particles at 0.05 m height. Zou et al. (2001) and Lü and Dong (2011) determined, by means of wind tunnel simulations, that the maximum kinetic energy of abrasion occurs at about 0.06 m above the soil surface.

The average speed of the particles mobilized by saltation (μ_p) was determined by the empirical equation (5) developed by Yang et al. (2007),

$$\mu_p(z) = \left(1.12 + \frac{0.13}{GMD^2} + 49.2\mu^* - 326.69GMD^3\mu^*\right)\sqrt{z} \quad (5)$$

where μ^* is the friction wind velocity (m s^{-1}), GMD (mm) is the geometric mean diameter of the saltating particles, z (m) is the height at which the speed of the particle was measured.

The average mass of the saltating particles (m) was determined with the Eq. (6),

$$m = Dr \times Vol \quad (6)$$

where Dr is the real average density in g cm^{-3} (Klute, 1986), and Vol is the average volume in cm^3, calculated by means of Eq. (7),

$$Vol = \left[4/3 \times 3.14 \times (GMD/2)^3\right]/1000 \quad (7)$$

where GMD is the geometric mean diameter of the saltating particles in mm.

2.2. Wind tunnel facility

For this study we used an 8 m-long wind tunnel. The simulation section of the tunnel is 6 m-long, 1 m-high and 0.5 m-wide. The working section, where soil samples are placed, is 4 m-long and the clean section is 2 m-long (Fig. 3). The soil bed consists of a 0.2 m-wide and 0.025 m-deep tray placed along the wind tunnel working section. For this study, the sides of the soil bed were covered with a coarse emery cloth, simulating rough conditions of the soil surface.

In the wind tunnel the air is pushed by an axial fan located before the clean section. The fan is driven by a Honda GX670 engine. Between the fan and the clean section there is a flow conditioning section (van Pelt et al., 2010) with several structures that allow a laminar flow of the air and boundary layer conditions. More details of the wind tunnel construction and the results of the wind tunnel calibration can be found in Mendez et al. (2006, 2011).

An abrader feeder was installed at the top of the tunnel, in the middle of the clean section. This device allowed the supply of the saltation fraction of each soil by gravity, at a mean flow rate of 0.0055 kg m^{-1} s^{-1} (van Pelt et al., 2010). The saltation material entered to a 1 cm wide tube located in the center of the tunnel section, which produced the material to fall from a height of 0.15 m.

The wind speed was measured with a pressure anemometer at 0.05, 0.17, 0.315, and 0.48 m high in order to determine the wind profile. These data were obtained within the boundary layer (height at which the logarithmic wind speed profile attains 99% of its maximum value), estimated between 0.4 y 0.6 m-high (Maurer et al., 2006; van Pelt et al., 2010). These measurements allowed the calculation of the friction velocity (Roney and White, 2006) with Eq. (8),

$$\mu^* = \frac{K(\mu_{Z_2} - \mu_{Z_1})}{\ln(Z_2 - Z_1)} \quad (8)$$

where μ^* is the wind friction speed in m s^{-1}, K is the von Karman constant (0.4), μ_{Z1} and μ_{Z2} are the wind velocities at Z_1 and Z_2 heights (0.005 and 0.48 m, respectively).

The wind erosion process was simulated under three different saltation conditions: injected saltation (IS), in which the saltation fraction of each soil was added to the soil bed, no saltation (NS), in which the soil, without injection of its saltation fraction, eroded naturally, and only saltation (OS), in which only the saltation fraction was injected, in absence of the soil sample in the working section. The isolated effect of IS on erosion was calculated with the difference between IS and OS. The whole soil, including its saltation fraction, was placed in the working section for simulations carried out for IS and NS treatments.

Wind tunnel simulations lasted 4 min and were performed at an average friction velocity of 0.21 m s^{-1} (standard deviation of 0.05). The short time used for simulations allowed relative stable conditions during the experiments (wind velocity, horizontal mass flux, amount of material supplied from the abrasion feeder, depletion of the original soil bed). IS and NS treatments were replicated 4 times, and OS 3 times. This was decided considering that the variation between replicates in OS was low (variation coefficient <15%).

The freestream velocity, measured at 0.7 m high, was similar in all three treatments, being 7.8 m s^{-1} in both, IS and NS (SD = 0.39 and 0.37, respectively), and 8.1 m s^{-1} in OS (SD = 0.31). These results indicate that the freestream velocity was rather constant in all treatments and that it was not affected by the presence or absence of saltators within the wind tunnel.

The material mobilized by saltation during wind tunnel simulations was collected with BSNE samplers (Fryrear et al., 1998) located at five different heights (0.05, 0.17, 0.315, 0.48 and

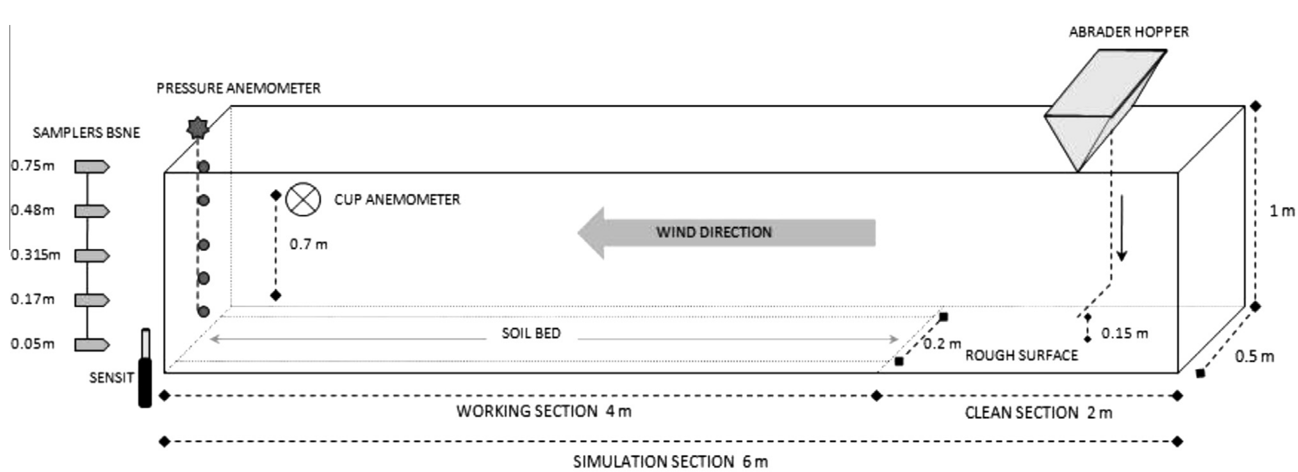

Fig. 3. Scheme of the working section of the wind tunnel.

0.75 m) at the end of the wind tunnel. In order to prevent interferences of BSNE traps on the determination of wind speeds, both instruments were placed at same heights but 0.1 m apart from each other.

The BSNEs collected material after each simulation was weighed. Such data were used for calculating the horizontal mass flux (Q), which was determined by the integration of the negative exponential curve that fitted Q vs height between 0 and 1 m high (Eq. (9)). This calculation was made by means of the Curve Expert® 1.3 software (Hyams, 2005).

$$Q = a\exp(bz) \quad (9)$$

where Q is the horizontal mass at height z, a is the flow of mass on the surface ($z = 0$) and b represents the rate of decay of the horizontal mass with height. Details on this method can be found in Panebianco et al. (2010).

The relationships between different variables were analyzed by means of linear and non linear regression analysis. The differences between the rates of erosion for each soil in the different treatments were analyzed by means of Tuckey mean comparison tests, using $\alpha = 0.05$. This analysis was performed by means of the INFOSTAT software (Di Rienzo et al., 2002).

3. Results and discussion

Table 2 shows that coarse textured soils (S1 and S2) had a saltation fraction with higher abrasion energy than fine textured soils. This is in agreement with the higher density of its saltating particles. As a matter of fact, a positive and linear correlation was found between sand contents and the abrasion energy (R^2: 0.96; $p < 0.001$).

The geometric mean diameter of the saltation fraction (GMD) shows lower values than the lower size of the saltation fraction (0.2 mm). This is because the determination of GMD was based on the granulometric analysis of this fraction with a particle laser counter, device that produces some dispersion of the sample and therefore some break-down of aggregates. This happens, even when samples preparation did not include a previous dispersion or destruction of the binding substances (organic matter and free lime). The separation of the saltation fraction was made by means of a gently hand dry sieving, process that reduced the destruction of aggregates. Despite this difference in the sizes, GMD values shown in Table 2 were used for the calculations of Eqs. (4) and (5), as they reflect the original composition of the saltating fraction.

The higher proportion of aggregates in the saltation fraction of fine textured soils and the lower proportion in sandy soils were confirmed by comparing the particle size distribution determined on samples with high and low dispersion pretreatments (Fig. 4). After the most energetic dispersion, the finest sized particles (<0.002 mm) increased less in sandy than in fine textured soils. Such increases were ordered in the sequence S1 < S3 < S5 < S6. In agreement with clay increases, most soils showed decreases of the coarsest fractions (0.05–2 mm). Such decreases tended to be higher in fine than in coarse textured soils. This indicates that the finest soils contained larger amounts of coarse aggregates than sandy soils. This agrees with findings of Buschiazzo and Taylor (1993) and Colazo and Buschiazzo (2014), who also demonstrated that coarse aggregates were more abundant in fine than in sandy textured soils. These authors attributed such tendencies to the low destruction of coarse aggregates occurring during the low-energy wind erosion transportation of fine aeolian materials that constitute the parent material of soils. Under these conditions, the collision between particles and the abrasion process should also have been low. The opposite occurred in sandy soils, in which the destruction of aggregates during wind transport processes was apparently higher, because the transport of sediments occurred under more energetic wind transport conditions.

Exceptions to the abovementioned general trends were S4 and S2, soils that showed, respectively, larger and lower increases of the finest particles after the high energetic dispersion treatment than expected for their textural composition. The behavior of these soils can be due to relative influence of OM on soil aggregation. In S4, OM contents were relatively high, producing a high proportion

Table 2
Parameters of the abrader energy of particles mobilized by saltation (Ø 0.2–0.5 mm) in each studied soil.

Soil	GMD mm	d g cm^{-3}	m g	μ_p m s^{-1}	Abrader energy Joule
S1	0.094	2.48	9.64E−07	5.84	1.64E−08
S2	0.074	2.47	4.65E−07	7.86	1.44E−08
S3	0.071	2.43	3.82E−07	8.32	1.32E−08
S4	0.094	2.24	8.33E−07	5.84	1.42E−08
S5	0.072	2.41	3.85E−07	8.16	1.28E−08
S6	0.040	2.19	3.94E−08	20.73	8.47E−09

GMD = geometric mean diameter; d: mean density of the saltation fraction; m: averaged mass of the saltating particles; μ_p is the average speed of the particles at 0.05 m height.

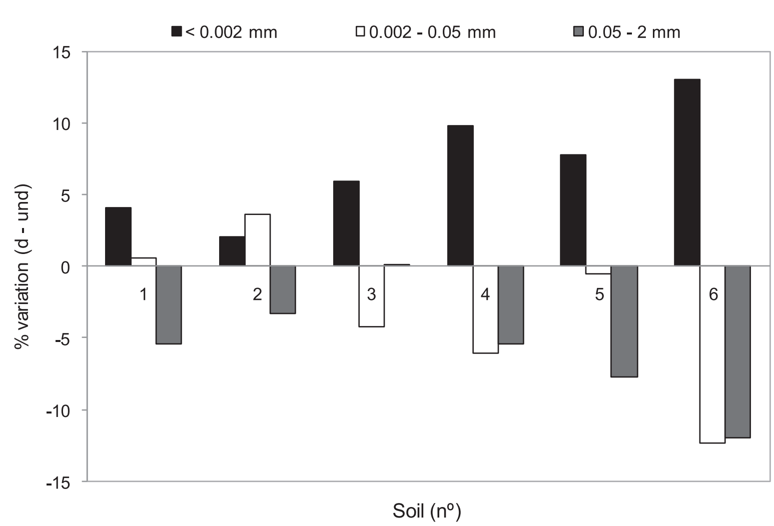

Fig. 4. Relative variation of clay (<0.002 mm), silt (0.002–0.05 mm) and sand (0.05–2 mm) of the saltation fraction between dispersed and less dispersed samples, in 6 soils.

of aggregates, despite its high sand contents. On the other hand, S2 contained relatively high amounts of OM but also high proportions of coarse sands, which lead to a lower aggregation rate than expected for its OM contents. The combined effect of OM and texture on the aggregation rate of the soils and its influence on the increase of fine particles after the high-energy dispersion treatment was confirmed by a linear regression analysis between clay increases after the high energetic dispersion correlated and the sum of silt, clay and OM ($R^2 = 0.78$; $p < 0.05$). This relationship indicates that the aggregation of fine textured soils is more affected by clay than by OM contents, while the opposite occurs in sandy soils. Fig. 5 also shows that the saltation fraction is composed mainly of aggregates in fine textured soils (S5 and S6) and of individual sand grains in sandy soils (S1 and S2). These results confirm that the disintegration of aggregates of the saltation fraction due to abrasion during the wind erosion process can be higher in fine that in coarse textured soils.

The combined positive effects of OM and clay contents on aggregation were also detected on other parameters derived from soil aggregation: the erodible fraction (EF, amount of aggregates smaller than 0.84 mm), and the dry aggregate stability (DSS) (Chepil, 1953). Fig. 6 shows that EF and DSS show logarithmic relationships with the coefficient "clay x OM", an index of the combined effect of both binding substances. The correlation was positive for DSS and negative for EF, indicating that the higher the contents of clay and OM the higher the aggregation of the soils. Similar results were found by other authors for the same soils than studied here (Buschiazzo et al., 1995; Colazo and Buschiazzo, 2010) and those of other regions (Skidmore and Layton, 1992; Öztas et al., 1999 and Djajadi et al., 2012). Soil 2 was not included in the regression showed in Fig. 6 because of its relatively high contents of >2 mm sized clasts that produced erroneous results during DSS and EF determinations with the rotary sieve. These clasts were resistant during the dry sieving, making DSS to be overestimated and EF to be underestimated in this soil.

Table 3 shows that wind erosion was higher in both, NS and IS, than in OS in all analyzed soils, averaging 11.93 $g\,m^{-2}\,s^{-1}$ in IS, 9.37 $g\,m^{-2}\,s^{-1}$ in NS and only 1.94 $g\,m^{-2}\,s^{-1}$ in OS. On average of all soils, erosion was 1.2 times higher in IS than in NS, which reflects the high influence of saltation on the erosion process.

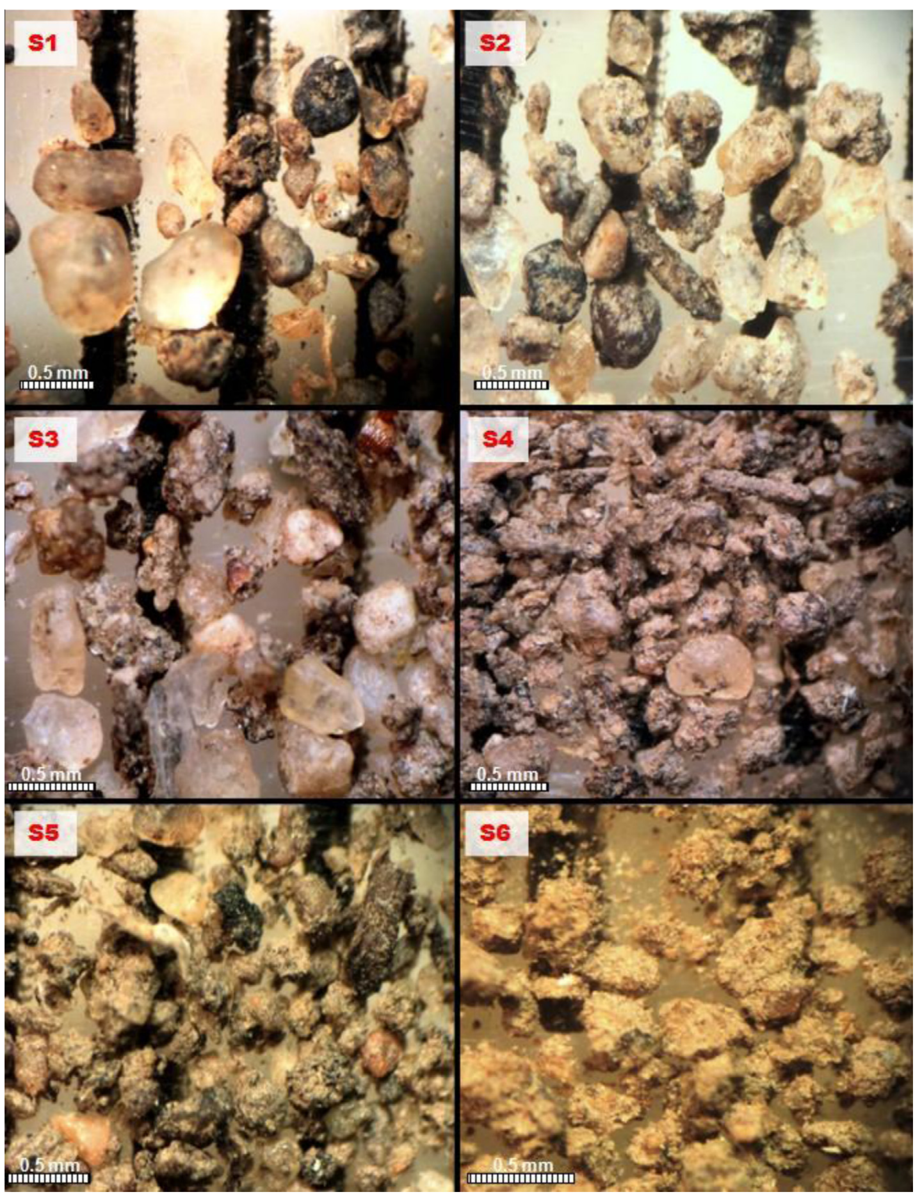

Fig. 5. Microphotographs of the saltation fraction of the studied soils.

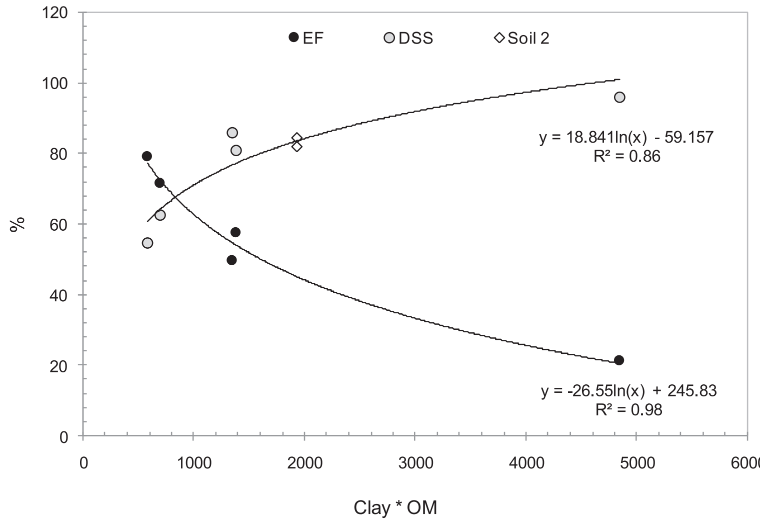

Fig. 6. Dry aggregate stability (DSS) and contents of the erodible fraction (EF) as a function of the product between clay and OM.

Table 3
Wind erosion (Q, g m^{-2} s^{-1}) under three different saltation conditions; injected saltation (IS), no saltation (NS), and only saltation (OS).

Treatment	Soils	S1	S2	S3	S4	S5	S6
	Q	20.35[a]	17.21[a]	15.85[a]	5.23[b]	6.62[b]	6.33[b]
IS	σ	2.21	2.86	3.58	0.71	0.71	0.74
(n = 24)	CV	10.87	16.59	22.59	13.58	10.78	11.74
	Q	18.67[a]	12.54[b]	13.03[b]	3.85[c]	5.02[c]	3.12[c]
NS	σ	3.77	1.44	2.12	0.59	0.85	0.86
(n = 24)	CV	20.17	11.45	16.23	15.22	16.85	27.67
	Q	2.39[a]	1.90[a]	2.18[a]	1.85[a]	2.10[a]	1.21[b]
OS	σ	0.11	0.27	0.12	0.16	0.29	0.07
(n = 18)	CV	4.58	14.34	5.48	8.70	13.80	5.63

Values with different letters indicate differences between soils within the same treatment ($p < 0.05$). σ is the standard deviation and CV is the coefficient of variation.

Soils with higher sand contents (S1, S2 and S3) showed erosion amounts three to four times higher than fine and well aggregated soils (S4, S5 and S6) in both, IS and NS. In OS, erosion was the same for all analyzed soils, in agreement with the similar supply of saltating material in all cases, with exception of S6, which showed low erosion. Low erosion amounts of S2 probably originated in the low efficiency of BSNE samplers to catch material transported by suspension, formed by the destruction of aggregates of the saltation fraction during wind erosion. It is widely known that BSNEs are designed for trapping saltation and not suspension fractions (Goossens and Buck, 2012; Sharratt et al., 2007; Shao et al., 1993a,b).

In NS, the average erosion amounts of coarse textured soils (S1, S2 and S3) was 14.75 g m^{-2} s^{-1}, while the same values for finer and better structured soils (S4, S5 and S6) was nearly four times lower (3.99 g m^{-2} s^{-1}). When the saltation fraction was injected (IS), differences between groups of soils remained, with averaged values of 17.8 g m^{-2} s^{-1} for sandy soils and 6.06 g m^{-2} s^{-1} for fine textured soils. In IS, the erosion of fine textured soils was approximately 33% lower than that of sandy soils, indicating that the additional injection of the saltation fraction had a differential effect on each soil type.

The increase of the erosion amount in IS with respect to NS, barely exceeded 20% in the coarse textured soils, and 50% in the more aggregated fine textured soils.

Fig. 7 shows how wind erosion amounts vary as a function of the abrader energy, corrected by the index of aggregation of the saltation fraction for IS and NS. The correlation was positive in both cases ($p < 0.05$; $p < 0.01$), indicating that the magnitude of wind erosion is determined not only by the abrader energy of the saltation fraction but also by the aggregation rate of the soil. The higher aggregation allowed the fine textured soils to resist better wind forces than sandy soils, with weaker aggregation. Wind erosion amounts of fine textured soils depend almost exclusively on the saltation process, while the low aggregation made sandy soils to be more dependent on their own properties.

The relative erosion (RE), the quotient between wind erosion amounts occurred in IS in relation to that of NS, can be considered an index of the relative effect of saltation on wind erosion. RE correlated positively ($p < 0.01$) with the quotient between the abrader energy and the index of aggregation of the saltation fraction deduced with Eq. (3). This correlation was also valid for the index alone (Fig. 8). Such correlations indicate that saltation affected more wind erosion in fine than in coarse textured soils. In sandy soils RE was close to 1, indicating that wind erosion that occurred in NS was similar to the one that occurred in IS. An increase in the kinetic energy of the saltation fraction produced a relatively small increment of the erosion in sandy soils, indicating that wind erosion occurred mainly because of the high susceptibility of the soil to be eroded by wind and not so much due to the energy of saltating particles streaking the soil surface. In fine textured soils, RE was near 2, indicating that saltation had a high effect on wind erosion. In these soils, probably, the fragmentation of aggregates by collision and abrasion of saltating aggregates and particles may have increased the amount of material transported by wind. According to Kun and Herrmann (1999), the transfer of kinetic energy onto an aggregate of bonded particles creates elastic waves within the aggregate that can break it down. Hagen (2004) found that the fragmentation of aggregates during the wind erosion process was higher when the silt contents also increased and that the relative breakdown of aggregates was greater in soils with a sand/clay ratios between 0.1 and 10. The finest textured soils (S5 and S6) showed high RE values and sand/clay ratios between 2.7 and 6.9, in agreement with Hagen (2004) results. Sandy soils presented sand/clay ratios higher than 10. Hagen (2004) argues that when a soil has a saltation fraction composed mainly of sand-sized particles (>100 μm diameter) it shows a limited amount of aggregates. Mirzamostafa et al. (1998) and Lyles and Tatarko (1986) suggest that the rate of aggregates that break down during saltation is inversely proportional to their clay contents.

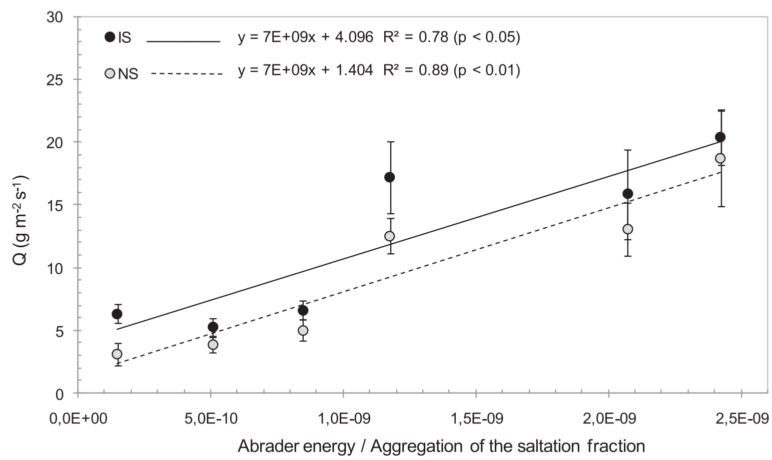

Fig. 7. Erosion amounts (*Q*) as a function of the quotient between the abrader energy and the aggregation of the saltation fraction of each soil, under two saltation conditions, injected saltation (IS) and no saltation (NS). Error bars represent the standard deviation of each point.

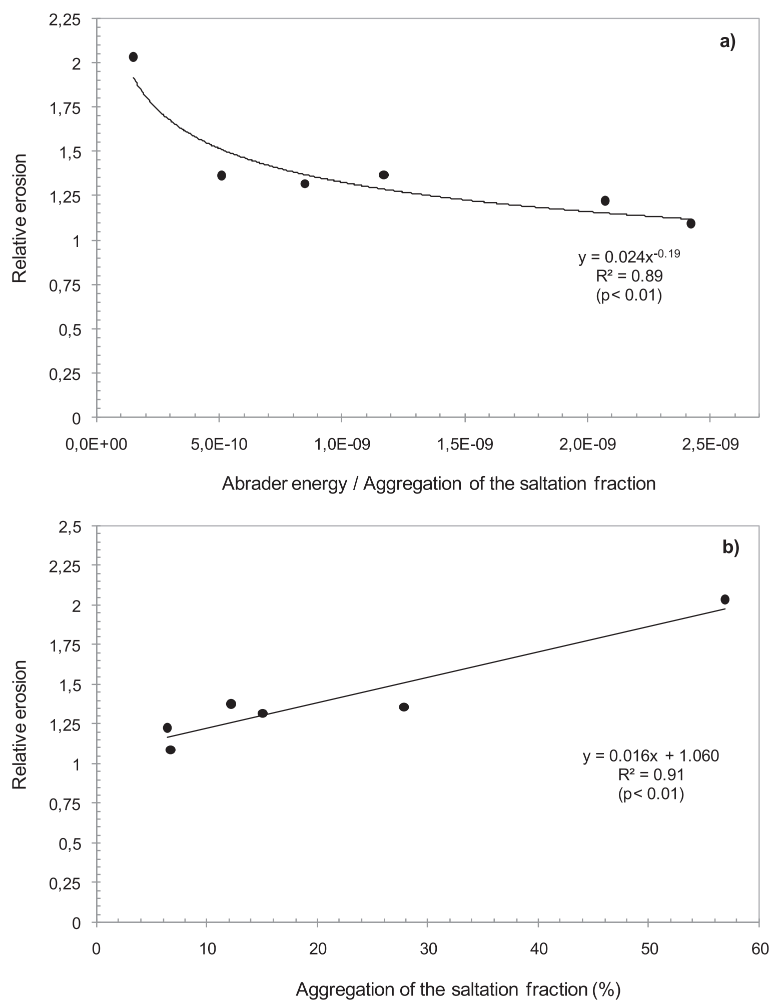

Fig. 8. Relative erosion (IS/NS) as a function of: (a) the quotient between the abrader energy and the aggregation index of the saltation fraction, and (b) the aggregation index of the saltation fraction.

4. Conclusions

Sandy soils presented a saltation fraction composed mainly of sand grains with higher density and kinetic energy than aggregates that composed, to a large extent, the saltation fraction of fine textured soils.

Wind erosion was more dependent on soil surface properties (low EF and DSS) in sandy soils and from the breakdown of aggregates during saltation in fine textured soils. This was confirmed by: (a) the high influence of saltation on the relative erosion amounts (the quotient between the erosion that occurred with and without saltation) in fine textured soils, and the lack of effect of saltation in sandy soils, and (b) the increase of wind erosion with increasing proportions of sand and decreasing silt, clay, and organic matter contents of the soils.

Acknowledgments

This study was financed by CONICET (PIP 2011-2013, No 0017), and ANPCyT (PICT 2011 No 354), Argentina, and INTA (National Soil Program).

References

Alfaro, S.C., 2008. Influence of soil texture on the binding energies of fine mineral dust particles potentially released by wind erosion. Geomorphology 93, 157–167.
Alfaro, S.C., Gomes, L., 2001. Modeling mineral aerosol production by wind erosion: emission intensities and aerosol distributions in source areas. J. Geophys. 106, 18,075–18,084.
Alfaro, S.C., Gaudichet, A., Gomes, L., Maillé, M., 1997. Modeling the size distribution of a soil aerosol produced by sandblasting. J. Geophys. Res. 102, 11,239–11,249.
Baas, A.C.W., 2004. Evaluation of saltation flux impact responders (Safires) for measuring instantaneous aeolian sand transport intensity. Geomorphology 59, 99–118.
Bagnold, R.A., 1941. The Physics of Blown Sand and Desert Dunes. Chapman and Hall, Methuen.
Barchyn, T.E., Hugenholtz, C.H., 2010. Field comparison of four piezoelectric sensors for detecting aeolian sediment transport. Geomorphology 120, 368–371.
Barchyn, T.E., Hugenholtz, C.H., Li, B., McKenna Neuman, C., Sanderson, R.S., 2014. From particle counts to flux: wind tunnel testing and calibration of the 'Wenglor' aeolian sediment transport sensor. Aeolian Res. 15, 311–318.
Bauer, B.O., Houser, C.A., Nickling, W.G., 2004. Analysis of velocity profile measurements from wind-tunnel experiments with saltation. Geomorphology 59, 81–98.
Bridges, N.T., Phoreman, J., White, B.R., Greeley, R., Eddlemon, E.E., Wilson, G.R., Meyer, C.J., 2005. Trajectories and energy transfer of saltating particles onto rock surfaces: application to abrasion and ventifact formation on Earth and Mars. J. Geophys. Res. 110, E12004. http://dx.doi.org/10.1029/2004JE002388.
Buschiazzo, D.E., Taylor, V., 1993. Efecto de la erosión eólica sobre algunas propiedades de suelos de la región semiárida pampeana central. Ciencia del Suelo 10 (11), 46–53.
Buschiazzo, D.E., Aimar, S.B., Stahr, K., 1995. Factores que afectan la estabilidad estructural de suelos de la Región Semiárida Pampeana Central (Argentina). Ciencia del Suelo 13, 66–69.
Cheng, H., Xue-Yong, Z., Chun-Lai, Z., Zhan-Jun, Q., 2009. Fall velocities of saltating sand grains in air and their distribution laws. Powder Technol. 192, 99–104.
Chepil, W.S., 1953. Factors that influence clod structure and erodibility of soil by wind: I. Soil texture. Soil Sci. 75, 473–483.
Chepil, W.S., 1962. A compact rotary sieve and the importance of dry sieving in physical soil analysis. Soil Sci. Soc. Am. Proc. 26, 4–6.
Colazo, J.C., Buschiazzo, D.E., 2010. Soil dry aggregate stability and wind erodible fraction in a semiarid environment of Argentina. Geoderma 159, 228–236.
Colazo, J.C., Buschiazzo, D.E., 2014. The impact of agriculture on soil texture due to wind erosion. Land Degrad. Develop. 26, 62–70.
Creyssels, M., Dupont, P., Ould El Moctar, A., Valance, A., Cantat, I., Jenkins, J.T., Pasini, J.M., Rasmussen, K.R., 2009. Saltating particles in a turbulent boundary layer: experiment and theory. J. Fluid Mech. 625, 47–74.
Di Rienzo, J.A., Casanoves, F., Balzarini, M.G., González, L., Tablada, M., Robledo, C.W., 2002. InfoStat versión 1.1. FCA, Universidad Nacionalde Córdoba.
Dietrich, R.V., 1977. Impact abrasion of harder by softer materials. J. Geol. 85, 242–246.
Djajadi, Abbott, L.K., Hinz, C., 2012. Synergistic impacts of clay and organic matter on structural and biological properties of a sandy soil. Geoderma 183–184, 19–24.
Dong, Z.B., Liu, X.P., Li, F., Wang, H.T., Zhao, A.G., 2002. Impact–entrainment relationship in a saltating cloud. Earth Surf. Process. Landforms 27, 641–658.
Fryrear, D.W., Saleh, A., Bilbro, J.D., Schomberg, H.M., Stout, J.E., Zobeck, T.M., 1998. Revised wind erosion equation (RWEQ). Technical Bulletin 1, Southem Plains Area Cropping Systems Research Laboratory, Wind Erosion and Water Conservation Research Unit, USDA-ARS.
Goossens, D., Buck, B.J., 2012. Can BSNE (big spring number eight) samplers be used to measure PM10, respirable dust, PM2.5 and PM1.0? Aeolian Res. 5, 43–49.
Greeley, R., Leach, R.N., Williams, S.H., White, B.R., Pollack, J.B., Kfinsley, D.H., Marshall, J.R., 1982. Rate of wind abrasion on Mars. J. Geophys. Res. 87, 10009–10024.
Grini, A., Zender, C.S., 2004. Roles of saltation, sandblasting, and wind speed variability on mineral dust aerosol size distribution during the Puerto Rican Dust Experiment (PRIDE). J. Geophys. Res. 109, D07202. http://dx.doi.org/10.1029/2003JD004233.
Hagen, L.J., 1984. Soil aggregate abrasion by impacting sand and soil particles. Trans. ASAE 27, 805–808.
Hagen, L.J., 1991. Wind erosion mechanics: abrasion of aggregated soil. Trans. ASAE 34, 831–837.
Hagen, L.J., 2004. Fine particulate (PM10 and PM 2.5) generated by breakage of mobile aggregates during simulated wind erosion. Trans. ASAE 47, 107–112.
Hagen, L.J., Skidmore, E.L., Layton, J.B., 1988. Wind erosion abrasion: effects of aggregate moisture. Trans. ASAE 31, 725–728.
Hyams D.G., 2005. Curve expert 1.37. A compressive curve fitting package for windows, Hixson, USA.
Klute, A., 1986. Methods of Soil Analysis, 2nd ed. ASA and SSSA, Madison, Wisconsin, USA, vol. 1, 188p.
Kok, J.F., Parteli, E.J.R., Michaels, T.I., Karam, D.B., 2012. The physics of wind-blown sand and dust. Rep. Prog. Phys. 75, 72pp.
Kun, F., Herrmann, H.J., 1999. Transition from damage to fragmentation in collision of solids. Phys. Rev. E 59, 2623–2632.
López, M.V., de Dios Herrero, J.M., Hevia, G.G., Gracia, R., Buschiazzo, D.E., 2007. Determination of the wind-erodible fraction of soils using different methodologies. Geoderma 139, 407–411.
Lü, P., Dong, Z., 2011. Horizontal momentum and kinetic energy loss of airflow near the surface of sandy beds. Sediment. Geol. 234, 116–119.
Lyles, L., Tatarko, J., 1986. Wind erosion effects on soil texture and organic matter. J. Soil Water Conserv. 41, 191–193.
Marticorena, B., Bergametti, G., 1995. Modeling the atmospheric dust cycle: 1. Design of a soil-derived dust emission scheme. J. Geophys. Res. 100, 16415–16430.
Maurer, T., Hermann, L., Gaiser, T., Mounkaila, M., Stahr, K., 2006. A mobile wind tunnel for wind erosion field measurements. J. Arid Environ. 66 (2), 257–271.
Mendez, M.J., De Dios Herrero, J.C., Buschiazzo, D.E., 2006. Desarrollo de un túnel de viento portátil para la medición de erosión eólica: XX Congreso Argentino de la Ciencia del Suelo, Salta-Jujuy, p. 371.
Mendez, M.J., Funk, R., Buschiazzo, D.E., 2011. Field wind erosion measurements with big spring number eight (BSNE) and modified wilson and cook (MWAC) samplers. Geomorphology 129, 43–48.
Mirzamostafa, N., Hagen, L.J., Stone, L.R., Skidmore, E.L., 1998. Soil aggregate and texture effects on suspension components from wind erosion. Soil Sci. 62, 1351–1361.
Öztas, T., Canpolat, M.Y., Sonmez, K., 1999. Strength of individual soil aggregates against crushing forces II. Influence of selected soil properties. Turk. J. Agric. Forestry 23, 573–577.
Panebianco, J.E., Buschiazzo, D.E., Zobeck, T.M., 2010. Calculation of the horizontal mass flux with different models for wind erosion quantification purposes. Earth Surf. Process. Landforms 35, 1548–1555.
Perfect, E., Kay, B.D., da Silva, A.P., 1995. Influence of soil properties on the statistical characterization of dry-aggregate strength. Soil Sci. Soc. Am. J. 59, 532–537.
Rice, M.A., Mcewan, I.K., 2001. Crust strength: a wind tunnel study of the effect of impact by saltating particles on cohesive soil surfaces. Earth Surf. Process. Landforms 26, 721–733.
Roney, J.A., White, B.R., 2006. Estimating fugitive dust emission rates using an environmental boundary layer wind tunnel. Atmos. Environ. 40, 7668–7685.
Schlichting, E., Blume, H., Stahr, K., 1995. Bodenkundliches Praktikum. P. Parey Verlag, Stuttgart, 195 pp.
Shao, Y., 2008. Physics and Modelling of Wind Erosion. Atmospheric and Oceanographic Sciences Library. Springer.
Shao, Y., Raupach, M.R., Findlater, P.A., 1993a. Effect of saltation bombardment on the entrainment of dust by wind. J. Geophys. Res. 98, 12719–12726.
Shao, Y., McTainsh, G.H., Leys, J.F., Raupach, M.R., 1993b. Efficiencies of sediment samplers for wind erosion measurement. Aust. J. Soil Res. 31, 519–532.
Shao, Y., Raupach, M.R., Leys, J.F., 1996. A model for predicting aeolian sand drift and dust entrainment on scales from paddock to region. Aust. J. Soil Res. 34, 309–342.
Sharratt, B., Feng, G., Wendling, L., 2007. Loss of soil and PM10 from agricultural fields associated with high winds on the Columbia Plateau. Earth Surf. Process. Landforms 32, 621–630.
Skidmore, E.L., Layton, J.B., 1992. Dry-soil aggregate stability as influenced by selected soil properties. Soil Sci. Soc. Am. J. 56, 557–561.
Skidmore, E.L., Hagen, L.J., Armburst, D.V., Durar, A.A., Fryrear, D.W., Potter, K.N., Wagner, L.E., Zobeck, T.M., 1994. Methods for investigating basic processes and conditions affecting wind erosion. In: Lal, R. (Ed.), Soil Erosion Research Methods. Soil & W. Cons. Soc, Ankeny, USA, pp. 295–330.
Soil Survey Division Staff, 1993. Soil survey manual. Soil conservation service. U.S. Department of Agriculture Handbook 18, Washington, DC.
Stockton, P.H., Gillette, D.A., 1990. Field measurement of the sheltering effect of vegetation on erodible land surfaces. Land Degrad. Rehabil. 2, 77–85.
Ta, Wanquan, 2007. Study of the energy abrasion rates of five soil types subject to oblique impacts. Geoderma 140, 97–105.
Van Pelt, R.S., Zobeck, T.M., Baddock, M.C., Cox, J.J., 2010. Design, construction, and calibration of a portable boundary layer wind tunnel for field use. Trans. ASABE 53, 1413–1422.
Yang, Ping, Dong, Zhibao, Qian, Guangqiang, Luo, Wanyin, Wang, Hongtao, 2007. Height profile of the mean velocity of an Aeolian saltating cloud: wind tunnel measurements by particle image velocimetry. Geomorphology 89, 320–334.
Zou, X.Y., Wang, Z.L., Hao, Q.Z., Zhang, C.L., Liu, Y.Z., Dong, G.R., 2001. The distribution of velocity and energy of saltating sand grains in a wind tunnel. Geomorphology 36, 155–165.